# Adaptive Threshold Edge Detection Algorithm Based on APDCSF and Anti-symmetrical Biorthogonal Wavelet Transform

Xiao Zhou, Xiaoyan Wang, Baochen Jiang, and Chengyou Wang
School of Mechanical, Electrical and Information Engineering, Shandong University, Weihai 264209, China
Email: zhouxiao@sdu.edu.cn; swwxy00800313@163.com; jbc@sdu.edu.cn; wangchengyou@sdu.edu.cn

***Abstract*** —This paper proposes an edge detection algorithm based on adaptive threshold which is obtained by histogram matching edge gradient value. The implementation of this algorithm is made up of three procedures: all phase discrete cosine sequency filtering, wavelet decomposition and adaptive threshold processing. The image is decomposed into low frequency and high frequency subbands by using all phase discrete cosine sequency filter (APDCSF). Experimental results on test images reveal that compared with the edge detection algorithm based on artificial threshold, the proposed one can create dynamic threshold adaptively and show better edge detection performance especially in terms of edge positioning accuracy.

***Index Terms***—Image processing, edge detection, all phase discrete cosine sequency filter (APDCSF), wavelet decomposition, adaptive threshold, artificial threshold

## I. Introduction

Edge is the basis of analyzing and understanding the image. Edge detection has important research value in image segmentation [1], image recognition, and image coding area etc. How to design optimal linear filters for image edge detection has been a popular research subject for all the time [2]. Hou *et al*. [3] proposed all phase discrete cosine sequency filter (APDCSF) for all phase subband decomposition of image. With the strict complementary property of the subbands divided by the APDCSF, only one low pass filter template is designed in the decomposition of each layer. Because of excellent time-frequency local and multiresolution analysis characteristics, wavelet transform is widely used in signal and image processing. Liu *et al*. [4] constructed anti-symmetrical biorthogonal wavelet filter banks with the same even length, the differential operator property of which was also analyzed. In this paper, we combine APDCSF and anti-symmetrical biorthogonal wavelet filter banks with the same even length to decompose image.

Many edge detection algorithms need various parameters. There are two fundamental parameters in extraction of edge features and determination of edge points: scale parameter and thresholding parameter [5]. Here we focus on the selection of thresholding parameter. The edge detection algorithm based on adaptive threshold which is obtained by histogram matching edge gradient value is proposed in the paper. The implementation of this algorithm consists of three procedures: all phase discrete cosine sequency filtering, wavelet decomposition and adaptive threshold processing. Experimental results reveal that compared with the edge detection algorithm based on artificial threshold, the proposed one shows better edge detection performance especially in terms of edge positioning accuracy.

The rest of this paper is organized as follows. Section II introduces construction of all phase discrete cosine sequency filter. Mallat algorithm for wavelet decomposition is explained in Section III. And then in Section IV, the threshold detection method by histogram matching edge gradient value is introduced. The program flow chart of edge detection algorithm based on adaptive threshold is described in detail. Experimental results and comparisons between the edge detection algorithm based on adaptive threshold and the one based on artificial threshold are given in Section V. Conclusion of the paper is given in Section VI.

## II. Construction of All Phase Discrete Cosine Sequency Filter

### A. All Phase Discrete Cosine Sequency Filtering

For a digital signal sequence $\{z(n)\}$, there are $N$ $N$-D vectors $\boldsymbol{Z}_i$ ( $i = 0,1,\cdots,N-1$ ) that contain $z(n)$ and have different intercepted phases [6]:

$$\begin{aligned}
[\boldsymbol{Z}_0]^{\mathrm{T}} &= [z(n-N+1), z(n-N+2), \cdots, z(n)], \\
[\boldsymbol{Z}_1]^{\mathrm{T}} &= [z(n-N+2), z(n-N+3), \cdots, z(n+1)], \\
&\vdots \\
[\boldsymbol{Z}_{N-1}]^{\mathrm{T}} &= [z(n), z(n+1), \cdots, z(n+N-1)].
\end{aligned} \tag{1}$$

Applying discrete cosine sequency filtering to each $N$-D vector in time domain, we get

$$\begin{aligned}
Y_L(i) &= \sum_{k=0}^{N-1} C^{\mathrm{T}}(i,k) \left\{ F(k) \sum_{j=0}^{N-1} C(k,j) Z_L(j) \right\} \\
&= \sum_{j=0}^{N-1} Z_L(j) \sum_{k=0}^{N-1} C^{\mathrm{T}}(i,k) C(k,j) F(k),
\end{aligned} \tag{2}$$

Manuscript received March 20, 2014; revised June 26, 2014.
This work was supported by the Fundamental Research Funds of Shandong University (Grant No. 2014ZQXM008).
Corresponding author email: zhouxiao@sdu.edu.cn.
doi:10.12720/jcm.9.6.515-520

where $\boldsymbol{C}$ and $\boldsymbol{C}^{\mathrm{T}}$ are DCT and IDCT transform matrices with size of $N \times N$ respectively, $\boldsymbol{F}$ means the sequency response vector with length of $N$, $\boldsymbol{Y}_L$ is the output vector of sequency filtering. Defining $H_i(j) = \sum_{k=0}^{N-1} C^{\mathrm{T}}(i,k)C(k,j)F(k),\ i,j = 0,1,\cdots,N-1$, we can get

$$Y_L(i) = \sum_{j=0}^{N-1} H_i(j)Z_L(j) = \langle \boldsymbol{H}_i, \boldsymbol{Z}_L \rangle \quad i = 0,1,\cdots,N-1. \tag{3}$$

For the same point $z(n)$, there are $N$ different filtering values: $Y_0(N-1), Y_1(N-2), \cdots, Y_{N-1}(0)$. In order to eliminate the different meanings of filtering values and reduce the blocking effects, we take the mean of these filtering values as the filtering response $y(n)$ of $z(n)$:

$$y(n) = \frac{1}{N}\sum_{i=0}^{N-1} Y_i(N-1-i) \tag{4}$$

According to (1), (3) and (4), we get

$$\begin{aligned} y(n) &= \frac{1}{N}\sum_{i=0}^{N-1}\sum_{j=0}^{N-1} H_{N-1-i}(j)Z_i(j) \\ &= \frac{1}{N}\sum_{i=0}^{N-1}\sum_{j=0}^{N-1} H_{N-1-i}(j)z(n-N+1+i+j) \\ &= \sum_{k=-(N-1)}^{N-1} Q(k)z(n-k) = Q(n) * z(n) \end{aligned} \tag{5}$$

$$\left.\begin{aligned} Q(n) &= \frac{1}{N}\sum_{m=n}^{N-1} H_m(m-n) \\ Q(-n) &= \frac{1}{N}\sum_{m=0}^{N-1-n} H_m(m+n) \end{aligned}\right\},\ n = 0,1,\cdots,N-1 \tag{6}$$

where $Q(n)$ is the unit impulse response of all phase discrete cosine sequency filter which is a kind of FIR filters with length of $2N-1$. It is easier to implement and can reduce blocking effects, which improves filtering performance effectively.

For one-dimensional all phase discrete cosine sequency filter, we can get

$$Q(n) = Q(-n),\ \ n = 0,1,\cdots,N-1 \tag{7}$$

According to (7), all phase discrete cosine sequency filter $\boldsymbol{Q}$ has the zero-phase characteristic. Suppose $\boldsymbol{Q}_{1/2} = [Q(0), Q(1), \cdots, Q(N-1)]^{\mathrm{T}}$, if we know $\boldsymbol{Q}_{1/2}$, $\boldsymbol{Q}$ can be obtained by using the symmetric property.

The design of all phase discrete cosine sequency filter of length $2N-1$ is composed of (7), (8) and (9):

$$\boldsymbol{Q}_{1/2} = \boldsymbol{V}\boldsymbol{F}, \tag{8}$$

$$V(m,n) = \begin{cases} \dfrac{N-m}{N^2}, & \text{for } m = 0,1,\cdots,N-1,\ n = 0, \\ \dfrac{\left[(N-m)\cos\dfrac{mn\pi}{N} - \csc\dfrac{n\pi}{N}\sin\dfrac{mn\pi}{N}\right]}{N^2}, & \\ & \text{for } m = 0,1,\cdots,N-1,\ n = 1,2,\cdots,N-1. \end{cases} \tag{9}$$

The design approach of one-dimensional all phase discrete cosine sequency filter can be extended to two-dimension. It can be proven that the all phase discrete cosine sequency filter $\boldsymbol{Q}$ with size of $N \times N$ also has the zero-phase characteristic by (10).

$$\begin{aligned} Q(m,n) = Q(m,-n) = Q(-m,n) = Q(-m,-n), \\ m = 0,1,\cdots,N-1,\ n = 0,1,\cdots,N-1. \end{aligned} \tag{10}$$

Apparently, if we know the lower right corner 1/4 of $\boldsymbol{Q}$, $\boldsymbol{Q}$ can be obtained by using the symmetric property.

For two-dimensional all phase discrete cosine sequency filter $\boldsymbol{Q}$, we can get

$$\boldsymbol{Q}_{1/4} = \boldsymbol{V}\boldsymbol{F}\boldsymbol{V}^{\mathrm{T}} \tag{11}$$

where $\boldsymbol{F}$ is the sequency response matrix with size of $N \times N$. Therefore the design method of $\boldsymbol{Q}$ is composed of (9)-(11).

### B. Selection of All Phase Discrete Cosine Sequency Filter

The selection of all phase discrete cosine sequency filter includes the selection of size and determination of transition zone.

The size of filter is selected by calculating the amount of computation which is mainly composed of multiplication operation. When we apply all phase discrete cosine sequency filter with size of $5 \times 5$ to image, the amount of computation for each pixel is $5 \times 5 = 25$. If all phase discrete cosine sequency filter with size of $7 \times 7$ is used, the amount of computation for each pixel is $7 \times 7 = 49$. And these two filters show close performance. Therefore, all phase discrete cosine sequency filter with size of $5 \times 5$ is selected in the paper.

The determination of filter transition zone is to distribute the high and low frequency subbands of filtering by experiments. The sequency response chosen in the paper is shown as follows:

$$F_{3\times3} = \begin{bmatrix} 1 & 0.3 & 0 \\ 0.3 & 0 & 0 \\ 0 & 0 & 0 \end{bmatrix}$$

Now we can compute the all phase discrete cosine sequency filter with size of $5 \times 5$ according to the design method above. The two-dimensional all phase discrete cosine sequency filter of zero-phase characteristic is shown below:

$$h_{5\times5} = \begin{bmatrix} 0.001 & 0.014 & 0.031 & 0.014 & 0.001 \\ 0.014 & 0.049 & 0.096 & 0.049 & 0.014 \\ 0.031 & 0.096 & 0.178 & 0.096 & 0.031 \\ 0.014 & 0.049 & 0.096 & 0.049 & 0.014 \\ 0.001 & 0.014 & 0.031 & 0.014 & 0.001 \end{bmatrix}$$

## III. Mallat Algorithm for Wavelet Decomposition

The flow chart of Mallat algorithm for finite length sequence $\{c_{j,k}\}$ is shown in Fig. 1 [7]. The decomposition algorithm can be written as

$$c'_{N-1,k} = \sum_{l=-N_1}^{N_2} \tilde{p}_l c_{N,k+l}, \quad d'_{N-1,k} = \sum_{l=-N'_1}^{N'_2} \tilde{q}_l c_{N,k+l} \tag{12}$$

$$c_{N-1,k} = c'_{N-1,2k}, \quad d_{N-1,k} = d'_{N-1,2k} \tag{13}$$

Take anti-symmetrical biorthogonal wavelet filter banks with the same even length Bior5.1 for example, the coefficients are as follows [4]:

$$\{\tilde{p}_k\} = \{\tilde{p}_{-2} \sim \tilde{p}_3\}$$
$$= \{0.0442,\ 0.2210,\ 0.4419,\ 0.4419,\ 0.2210,\ 0.0442\};$$
$$\{\tilde{q}_k\} = \{\tilde{q}_{-2} \sim \tilde{q}_3\}$$
$$= \{0.2652,\ 1.3258,\ 1.7678, -1.7678, -1.3258, -0.2652\};$$
$$\{p_k\} = \{p_{-2} \sim p_3\}$$
$$= \{0.2652, -1.3258,\ 1.7678,\ 1.7678, -1.3258,\ 0.2652\};$$
$$\{q_k\} = \{q_{-2} \sim q_3\}$$
$$= \{0.0442, -0.2210,\ 0.4419, -0.4419,\ 0.2210, -0.0442\}.$$

$$\{c_{N,k}\} = \{162,163,166,162,155,160,157,161\} \quad (L = 8)$$

is taken from Lena for wavelet decomposition and reconstruction processes, the flow charts of which are shown in Fig. 2.

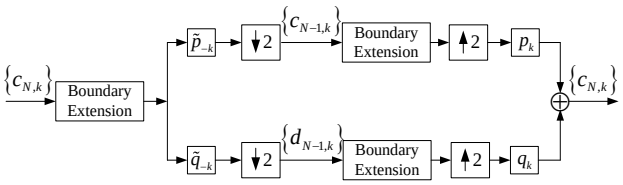


Fig. 1. Mallat algorithm of finite length sequence.

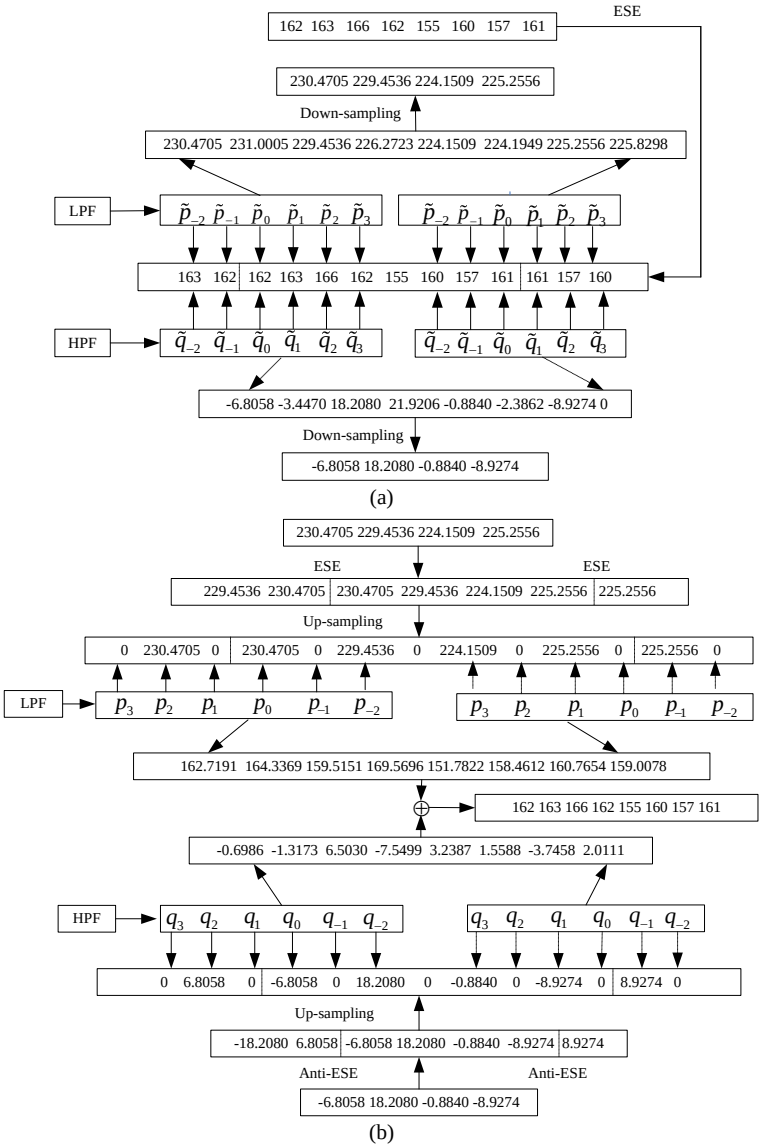


Fig. 2. An example of ESE with image data ( $L = 8$ ): (a) The decomposition process, (b) The reconstruction process.

## IV. Edge Detection Algorithm Based on Adaptive Threshold

### A. Threshold Detection by Histogram Matching Edge Gradient Value

After wavelet decomposition, four areas are derived: horizontal and vertical low frequency information (LL); horizontal high frequency and vertical low frequency information (HL); horizontal low frequency and vertical high frequency information (LH); horizontal and vertical high frequency information (HH) [8]. Since the HL and LH contain most of image details, they are selected for edge detection in the paper. Firstly, we compute the absolute values of high frequency data. Subsequently the high frequency data are extended to 200 and converted to integers as line amplitude. With the increase of line amplitude, the number of pixels becomes smaller, as shown in Fig. 3(a). Most places of the image changes gently. And there is no obvious boundary between the place changing dramatically and the one changing gently. Therefore we need to construct a mathematical model to fit it. With the properties of sharp dropping like histogram and obvious boundaries, the step function $g(s)$ in Fig. 3(b) fits Fig. 3(a) very well.

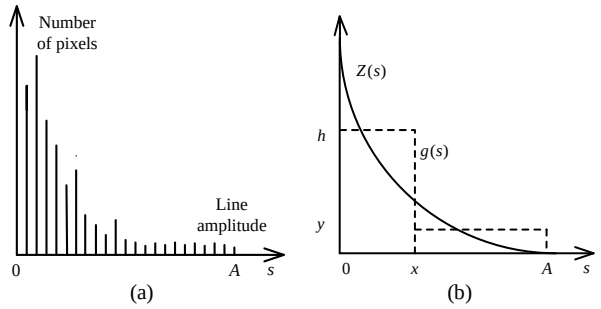


Fig. 3. Threshold detection by histogram matching edge gradient value: (a) Histogram, (b) The step function matching histogram.

If the shaking of histogram is ignored, monotonically decreasing $Z(s)$ is obtained, as shown in Fig. 3(b). In Fig. 3(b), the $s$ means the amplitude of gradient and the sample space is $[0, A]$. The $x$ means the coordinate of step point. The step function $g(s)$ is

$$g(s) = \begin{cases} h, & 0 \le s < x \\ y, & x \le s < A \end{cases} \tag{14}$$

If the area under the curve $Z(s)$ is $w$, to achieve the same total probability fit, the constraint condition satisfies:

$$\int_0^A Z(s)\mathrm{d}s = \int_0^A g(s)\mathrm{d}s = hx + y(A-x) = w \tag{15}$$

After derivation, we can get

$$f(x) = A(\eta - 2\omega\sigma) = 0 \tag{16}$$

where

$$v = \frac{w}{A}, \quad P = \frac{1}{A-x}\int_x^A Z(s)ds, \quad \omega = \frac{x}{A}, \quad \sigma = Z(x) - P,$$

$\eta = v - P$. Therefore, the coordinate of intersection point of $\eta$ and $2\omega\sigma$ is the solution of $f(x) = 0$ [6].

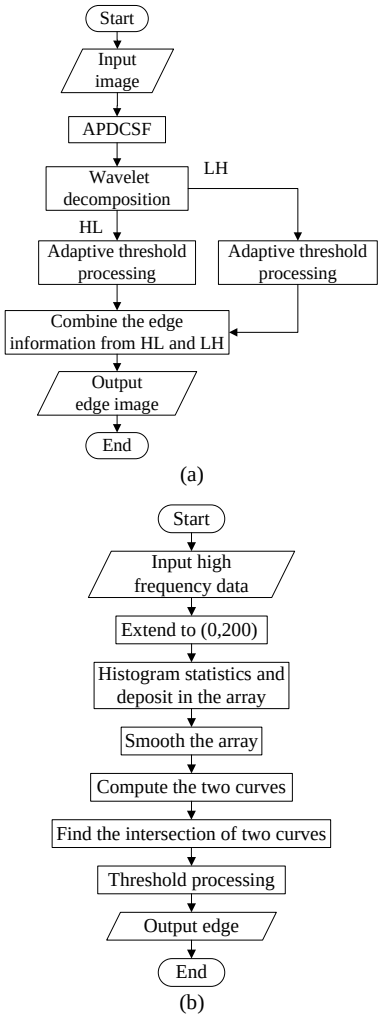


Fig. 4. Flow charts of edge detection algorithm based on adaptive threshold: (a) Main program, (b) Adaptive threshold processing.

### B. Process of Edge Detection Algorithm

Fig. 4(a) shows the main program flow chart of edge detection algorithm based on adaptive threshold. Firstly, all phase discrete cosine sequency filtering is applied to an image, which produces the low frequency and high frequency subbands. After wavelet decomposition to the low frequency subband, four areas are derived: LL, HL, LH and HH. Then the HL and LH are respectively performed with adaptive threshold processing. Finally, the edge information from HL and LH are combined for obtaining the edge image.

Adaptive threshold processing flow chart is shown in Fig. 4(b). Firstly, we compute the absolute values of high frequency data. Subsequently the high frequency data are extended to 200 and converted to integers. We proceed the histogram statistics according to the number of pixels which are equal to each value in $(0, 200)$ and deposit them in the array. After smoothing the array, the two curves $\eta$ and $2\omega\sigma$ are computed. Then we find the

intersection of two curves for obtaining threshold. Finally the high frequency data go through threshold processing to get edge.

The edge detection algorithm based on artificial threshold is similar to the adaptive one. The difference between them is adaptive threshold processing. Artificial threshold processing is introduced as follows. Firstly, the absolute values of high frequency data are computed. Then the high frequency data are extended to 200 and converted to integers. We choose $200/10$ as the threshold to proceed threshold processing for getting edge.

## V. Experimental Results

In the paper, all experimental results are obtained with MATLAB 7.8. To test the proposed scheme and compare with edge detection algorithm based on artificial threshold, gray images Lena and Barbara with size of $512\times512$ are used in the experiments. Anti-symmetrical biorthogonal wavelet Bior5.1 is used in wavelet decomposition process.

(a) (b) (c)

Fig. 5. Image Lena and its edge detection results: (a) Original image Lena, (b) Artificial threshold method, (c) Adaptive threshold method.

Fig. 5 shows the original image Lena (Fig. 5(a)) and its edge detection results. Fig. 5(b) and Fig. 5(c) show Lena's edge images obtained by the edge detection algorithms based on artificial threshold and adaptive threshold respectively. Fig. 6 shows the original image Barbara (Fig. 6(a)) and its edge detection results. Fig. 6(b) and Fig. 6(c) show Barbara's edge images obtained by the edge detection algorithms based on artificial threshold and adaptive threshold respectively.

(a) (b) (c)

Fig. 6. Image Barbara and its edge detection results: (a) Original image Barbara, (b) Artificial threshold method, (c) Adaptive threshold method.

From the experimental results in Fig. 5 and Fig. 6, we can see that the performance of edge detection algorithm based on adaptive threshold is good in terms of edge detection comprehensiveness and edge positioning accuracy. In order to realize the best edge detection performance, the edge detection algorithm based on adaptive threshold can create dynamic threshold adaptively for different images. However, the edge detection algorithm based on artificial threshold shows poor performance especially in terms of edge positioning accuracy. Therefore, the performance of edge detection algorithm based on adaptive threshold is better than the one based on artificial threshold.

## VI. Conclusion

In this paper, the theory of all phase discrete cosine sequency filtering is introduced. The edge detection algorithm based on adaptive threshold consists of three steps: all phase discrete cosine sequency filtering, wavelet decomposition and adaptive threshold processing. Two edge detection algorithms based on artificial threshold and adaptive threshold are achieved. The experiments to typical test images are done in MATLAB tool. Compared with the edge detection algorithm based on artificial threshold, the one based on adaptive threshold can create dynamic threshold adaptively and show better edge detection performance especially in terms of edge positioning accuracy.

## Acknowledgment

This work was supported by the Fundamental Research Funds of Shandong University (Grant No. 2014ZQXM008), the Graduate Innovation Foundation of Shandong University at WeiHai (GIFSDUWH) (Grant No. yjs12028), the National Natural Science Foundation of China (Grant No. 61201371) and the promotive research fund for excellent young and middle-aged scientists of Shandong Province, China (Grant No. BS2013DX022). The authors would like to thank Fanfan Yang and Qiming Fu for their help and valuable suggestions. The authors also thank the anonymous reviewers and the editor for their valuable comments to improve the presentation of the paper.

## References

[1] Z. W. Ju, J. L. Zhou, X. Wang, and Q. Shu, "Image segmentation based on adaptive threshold edge detection and mean shift," in *Proc. 4th IEEE International Conference on Software Engineering and Service Science*, Beijing, China, 2013, pp. 385-388.

[2] Z. H. Li, Z. H. Yang, W. L. Wang, and J. G. Cui, "An adaptive threshold edge detection method based on the law of gravity," in *Proc. 25th Chinese Control and Decision Conference*, Guiyang, China, 2013, pp. 897-900.

[3] Z. X. Hou, C. Y. Wang, and A. P. Yang, "All phase biorthogonal transform and its application in JPEG-like image compression," *Signal Processing: Image Communication*, vol. 24, no. 10, pp. 791-802, Nov. 2009.

[4] J. Z. Liu, Z. X. Hou, and C. Y. Wang, "Design and properties of anti-symmetric biorthogonal wavelet filter banks with the same even length," in *Proc. International Conference on Wavelet Analysis and Pattern Recognition*, Baoding, China, 2009, pp. 319-323.

[5] T. Sugiyama and K. Abe, "Edge detection method based on edge reliability with fixed threshold: consideration of uniformity and gradation," in *Proc. 15th International Conference on Pattern Recognition*, Barcelona, Spain, 2000, pp. 656-659.

 

[6] Z. X. Hou and Y. C. Guo, "Sequency subband feature coding on 2-D APDCSF," *Journal of Optoelectronics Laser*, vol. 16, no. 9, pp. 1112-1117, Sep. 2005.
[7] Z. X. Hou, C. Y. Wang, and A. P. Yang, "Study on symmetric extension methods in Mallat algorithm of finite length signal," in *Proc. 5th International Conference on Visual Information Engineering*, Xi'an, China, 2008, pp. 341-346.
[8] Q. Yin, Z. Y. Yuan, Y. Kong, and P. Guo, "Face recognition research based on anti-symmetrical wavelet and eigenface," in *Proc. 6th International Conference on Machine Learning and Cybernetics*, Hong Kong, China, 2007, pp. 366-371.

**Xiao Zhou** was born in Shandong province, China in 1982. She received her B.E. degree in automation from Nanjing University of Posts and Telecommunications, China, in 2003, her M.E. degree in information and communication engineering from Inha University, Korea in 2005, and her Ph.D. degree in information and communication engineering from Tsinghua University, China in 2013. Now she is a lecturer in the School of Mechanical, Electrical and Information Engineering, Shandong University, Weihai, China. Her current research interests include wireless communication technology, image processing and transmission technology.

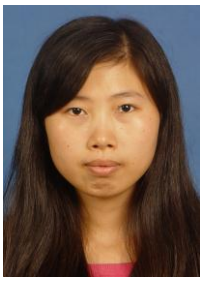

**Xiaoyan Wang** was born in Shandong province, China in 1990. She received her B.S. degree in electronic information science and technology from Shandong University, Weihai, China, in 2012. Now she is pursuing her M.E. degree in circuits and systems in Shandong University, Weihai, China. Her research interests concentrate on image and video processing.

**Baochen Jiang** was born in Shandong province, China in 1962. He received his B.S. degree in radio electronics from Shandong University, China, in 1983 and his M.E. degree in communication and electronic systems from Tsinghua University, China, in 1991. Now he is a professor in the School of Mechanical, Electrical and Information Engineering, Shandong University, Weihai, China. His current research interests include signal and information processing, image and video processing, and smart grid technology.

**Chengyou Wang** was born in Shandong province, China in 1979. He received his B.E. degree in electronic information science and technology from Yantai University, China, in 2004 and his M.E. and Ph.D. degree in signal and information processing from Tianjin University, China, in 2007 and 2010 respectively. Now he is an associate professor in the School of Mechanical, Electrical and Information Engineering, Shandong University, Weihai, China. His current research interests include image processing and transmission technology, multidimensional signal and information processing, and smart grid technology.